Organic & Biomolecular Chemistry
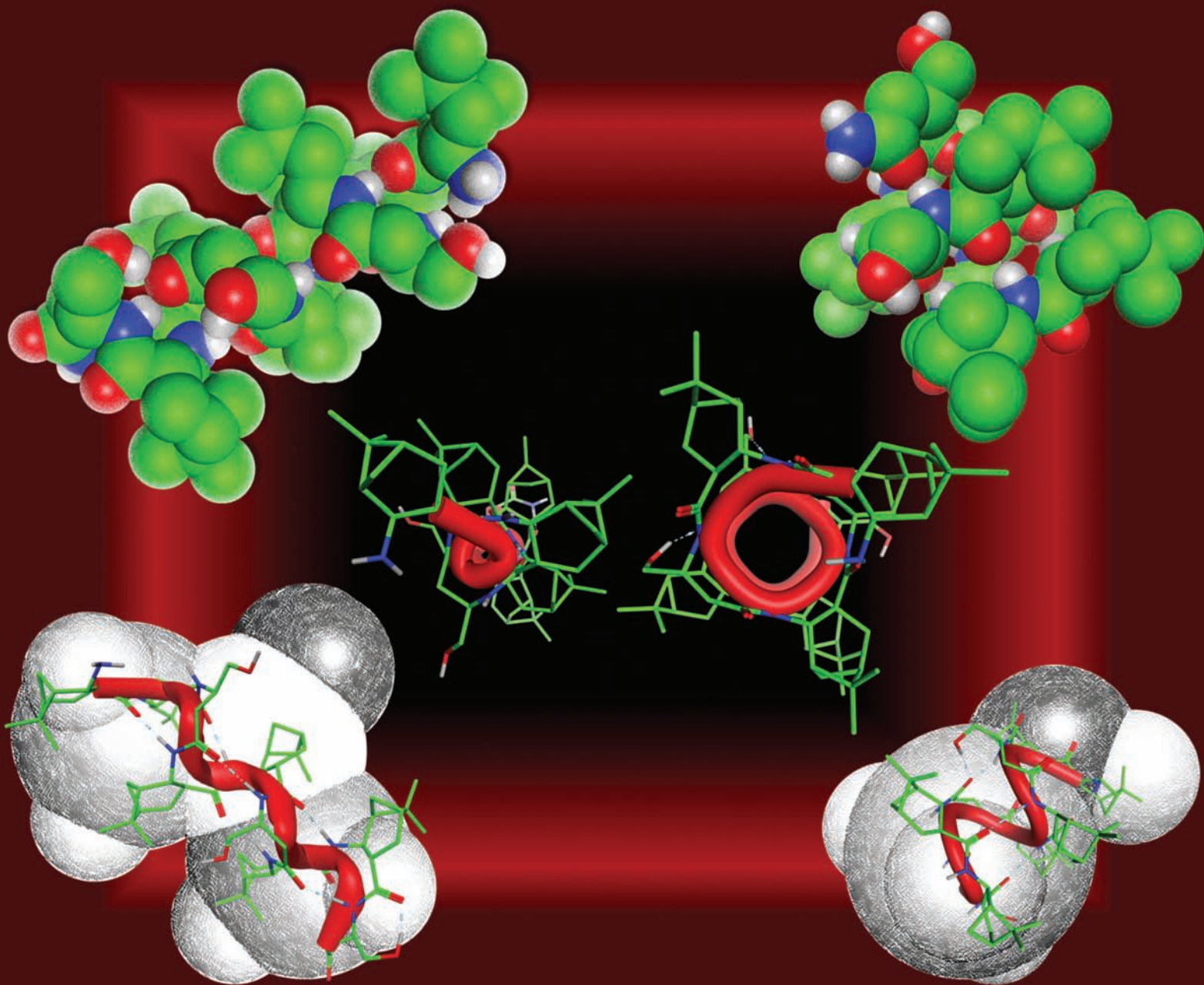
RSCPublishing

COMMUNICATION
Tamás A. Martinek *et al.*
Self-association-driven transition of the
β-peptidic H12 helix to the H18 helix

Self-association-driven transition of the β-peptidic H12 helix to the H18 helix†‡

Éva Szolnoki,[a] Anasztázia Hetényi,[b] Tamás A. Martinek,*[a] Zsolt Szakonyi[a] and Ferenc Fülöp[a]

Various patterns of foldameric oligomers formed by *trans*-ABHC ((1*S*,2*S*,3*S*,5*S*)-2-amino-6,6-dimethylbicyclo-[3.3.1]heptane-3-carboxylic acid) and β³-hSer residues were studied. NMR, ECD and molecular modelling demonstrated that octameric and nonameric sequences with multiple i–i+3 ABHC pair repulsions attain the β-H18 helix in CD₃OH. As a close relative of the α-helix, this helix type is stabilized by i–i+4 backbone H-bond interactions. The formation of the β-H18 helix was found to be solvent- and concentration-dependent. Upon dilution, the β-H18 → β-H12 helix transition was revealed by concentration-dependent ECD, DOSY-NMR and TEM measurements.

Introduction

Programmable folding and mimicry of the structural behaviour of biomolecules can be achieved with foldamers.[1–3] β- and αβ-peptides, the closest relatives of the natural α-peptides or proteins, occupy a distinguished position as the most thoroughly studied test bed.[4–8] Although foldamers obey rules similar to those governing the folding of biopolymers in many respects, there are distinct features that offer very efficient tools through which to control the secondary structure formation, *e.g.* cyclic side-chain constraints,[9–13] shape control[14–16] and backbone stereochemical configuration patterning for aliphatic peptide foldamers.[17–19] As concerns the tertiary/quaternary structure, similar behaviour has been observed: solvophobic interactions comprise the major driving force for the folding and self-assembly of the secondary structure units into higher-order structures.[20–25] In these foldameric tertiary structures, the cooperative folding is accompanied by a concentration-dependent transition from random coil to helix secondary structures.

Conformational polymorphism, such as the random coil → helix[26,27] or the helix → helix[28,29] transition is an important feature

of biopolymers. It can be closely connected to the function, *e.g.* voltage-gated ion channels make use of the 3₁₀-helix → α-helix transition.[30] In this case the helix geometry is affected by the tertiary packing and the external stimulus. Control over the 3₁₀-helix–α-helix equilibria of artificial α-peptidic chains has been achieved in a concentration-dependent manner[31] and through change of the solvent polarity.[32] Conformational polymorphism has also been observed for peptidic foldamers.[33,34] The helix geometries were controlled by adjusting the chain length and the substitution pattern of the peptidic chain, but a system in which higher-order long-range interchain interactions induce a helix → helix transition has not been described.

We report here a concentration- and solvent-dependent helix → helix transition not previously observed for foldamers. These findings facilitated the discovery of the β-peptidic H18 helix, the β-peptidic helix with the largest diameter known to date.

Results and discussion

Our earlier results demonstrated the ability of the homooligomers of the apopinane-based β-amino acid (1*R*,2*R*,3*R*,5*R*)-2-amino-6,6-dimethylbicyclo[3.3.1]heptane-3-carboxylic acid (*trans*-ABHC)[35] to adopt a H12 helix.[16] The incorporation of ABHC (a bulky bicyclic analogue of ACHC) in the sequence causes steric clashes between the side-chains in positions i–i+3, which is a highly effective way to destabilize the H14 helix and to promote formation of the H12 helix. It is known that increase of the chain length can result in larger-diameter helices, such as the chain length-dependent transition from the 3₁₀-helix to the α-helix, from the β-H10 helix to the β-H14 helix[34] and from the αβ-H9/11 helix to the αβ-H14/15 helix.[36–39] Since the present system is not stable in the β-H14 helix conformation, larger diameter helices (*e.g.* β-H16 helix or β-H18 helix) were expected in response to elongation of the sequence. However, a longer chain length causes severe problems concerning the solubility of the pure ABHC chains, and we therefore opted for the insertion of open-chain hydrophilic β³-hSer into the sequence in various patterns (Fig. 1). In order to focus on the effects of the steric interactions, we avoided the application of charged side-chains that could potentially lead to salt–bridge interactions. In order to match stereochemical arrangement of the β³-hSer, (1*S*,2*S*,3*S*,5*S*)-ABHC was utilized.

The chain assembly was carried out on a solid support, by means of Fmoc chemistry and HATU/DIPEA coupling, without

[a]Institute of Pharmaceutical Chemistry, University of Szeged, Eötvös u. 6., H-6720 Szeged, Hungary. E-mail: martinek@pharm.u-szeged.hu; Fax: +36 62545705; Tel: +36 62545564

[b]Department of Medical Chemistry, University of Szeged, Dóm tér 8., H-6720 Szeged, Hungary

This journal is © The Royal Society of Chemistry 2012

Org. Biomol. Chem., 2012, **10**, 255–259 | 255
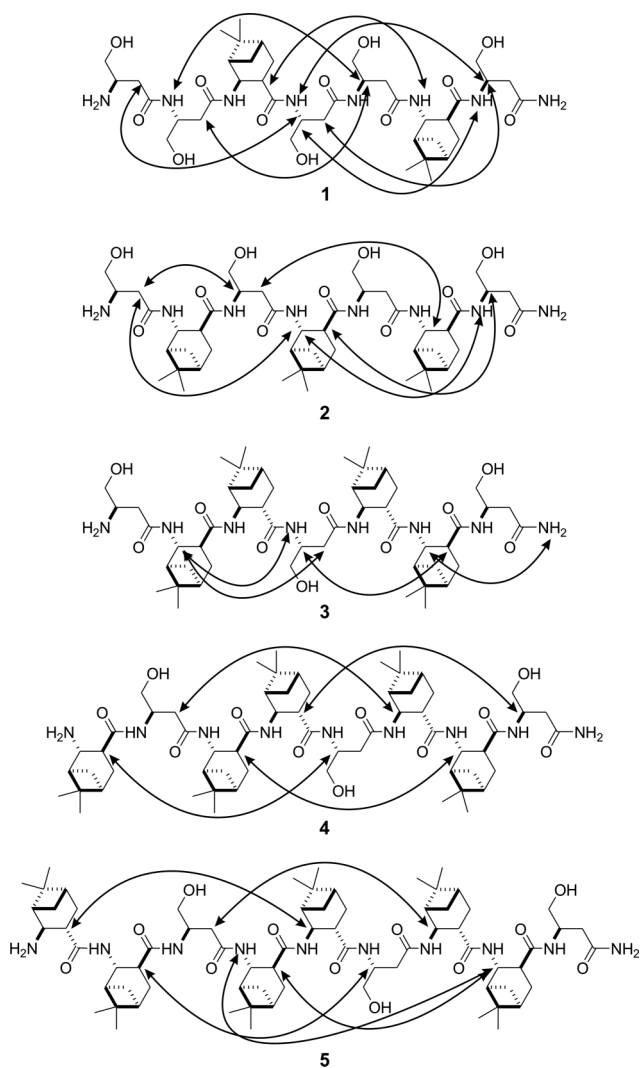
Fig. 1 Long-range NOE interactions observed for **1–5** in CD$_3$OH.

Fig. 2 ECD curves measured for **1** (black), **2** (green), **3** (dashed), **4** (blue) and **5** (red) in CH$_3$OH at a concentration of 1 mM.

difficulties. The peptides were detached from the resin with TFA–H$_2$O (95 : 5) solution. The products were isolated by RP-HPLC and characterized by means of MS. The signal dispersions were good enough to allow complete ^{1}H-NMR assignments along the backbone with the help of TOCSY and ROESY spectra recorded in the concentration range 1 mM–100 μM in [D$_6$]DMSO and CD$_3$OH. These foldamers were in general not water-soluble.

Electronic circular dichroism (ECD) spectra were recorded in CH$_3$OH at a foldamer concentration of 1 mM. Foldamers **1–3** displayed marked differences in their ECD fingerprints (Fig. 2). For **1**, a minimum near 215 nm and a maximum near 195 nm indicated a left-handed (M) β-H14 helix. A lower-intensity negative Cotton effect observed for **2** suggested partial folding to the β-H14 helix. For **3**, a positive Cotton effect with a high-wavelength lobe at around 220 nm was characteristic of a right-handed (P) β-H12 helix. These data suggest that one ABHC–ABHC pair in juxtaposition can be accommodated by the H14 helix, and two bulky residues are necessary in the i–i+3 position for rewinding into the β-H12 helix. Interestingly, **4** and **5** again exhibited a negative Cotton effect, but without the positive lobe seen at around

220 nm for **3**, and the negative lobe remained below 210 nm (Fig. 2). This indicates that **4** and **5** have opposite helicity to that of **3**. The helicity change could be explained by the formation of left-handed (M) β-H14 helices, but this is unlikely because of the higher number of ABHC–ABHC i–i+3 repulsions in **4** and **5**. The ECD findings pointed to the appearance of a new left-handed (M) helix type in CH$_3$OH for the octameric and nonameric sequences.

In order to acquire high-resolution structural data, ROESY experiments were run in CD$_3$OH and [D$_6$]DMSO. Signal-rich ROESY spectra were observed for **1** and **2** in CD$_3$OH; the characteristic C^{β}H$_i$–NH$_{i+3}$ and C^{α}H$_i$–C^{β}H$_{i+3}$ long-range NOE interactions supported the β-H14 helix (Fig. 1). A single C^{α}H$_i$–C^{β}H$_{i+2}$ long-range NOE interaction was found for **2**, indicating its less stable β-H14 helical conformation. The ROESY spectra for **1** and **2** in [D$_6$]DMSO were signal-poor, indicating that the chaotropic solvent was able to unfold the β-H14 helices. This was also reflected by the higher values of the negative temperature gradients of the amide protons $(-\Delta\delta/\Delta T)$[40] as compared with those of **3–5** (Fig. S18). On the other hand, numerous C^{β}H$_i$–NH$_{i+2}$ and C^{β}H$_i$–C^{α}H$_{i+2}$ NOE interactions were identified both in CD$_3$OH (Fig. 1) and in [D$_6$]DMSO, and contacts between the axial Me groups and amide protons (Me$_i$–NH$_{i+3}$) were also observed for **3**. Structure refinement calculations were carried out with the use of these NOE restraints, and the scalar coupling data strongly supported the formation of the well-folded right-handed (P) β-H12 helix (Fig. S19‡). The NMR results were in line with the ECD findings and indicated that the presence of at least two ABHC pairs in the i–i+3 positions is necessary to guide the system successfully into the β-H12 helix for these heptameric sequences.

The NOE patterns for **4** and **5** were solvent-dependent. While the known C^{β}H$_i$–C^{α}H$_{i+2}$ interactions were observed (indicative of the β-H12 helix) in [D$_6$]DMSO (Fig. S11‡), previously unreported NOE patterns appeared in CD$_3$OH. Long-range NOEs arising from C^{α}H$_i$–C^{β}H$_{i+4}$ interactions could be clearly identified (Fig. 1). The structure refinement led to the conclusion that this pattern can be explained by left-handed (M) β-H18 helix geometry, where the ABHC–ABHC repulsions are relieved. The comparison with the ECD results strongly indicated that elongation of the chain with additional ABHC residues leads to preference for the i–i+4 H-bonded β-H18 helices in CD$_3$OH. The structure refinement for **5** revealed that the NOE C^{β}H$_1$–C^{α}H$_6$ and

$C^\beta H_3$–$C^\alpha H_8$ cross-peaks in CD_3OH (Fig. S13‡) are not consistent with a self-contained helix; these interactions indicate head-to-tail helix contacts.

The lowest-energy conformers from the simulations of **4** and **5** were selected and further optimized at the *ab initio* quantum chemical level of theory.[41] The HF/3-21 level of theory in a vacuum was first utilized, as this has been reported to provide a good approximation to the geometry of the β-peptides.[42,43] The structures converged to the corresponding local minimum of the potential energy surface. To take into account the effects of more diffuse basis sets and the electron correlation, the optimizations were performed at the B3LYP/6-311G** level. The structure optimizations converged properly and the new foldameric left-handed (M) helices stabilized by 18-membered H-bonded rings were obtained (Fig. 3).
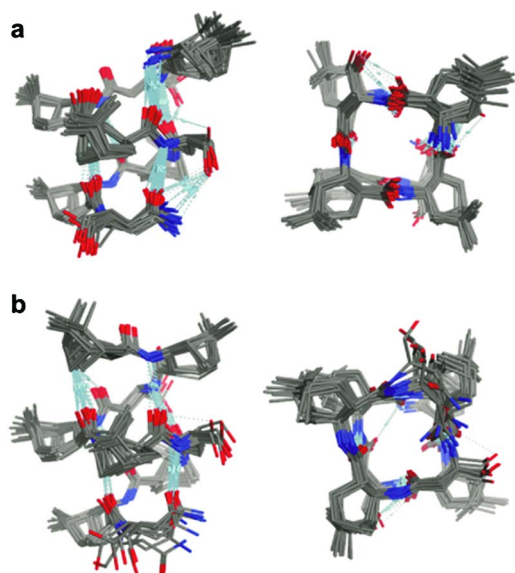

Fig. 3 Side and top views of the β-H18 helix obtained from the NMR structure refinement for **4** (a) and **5** (b) in CD_3OH.

Such a sharp chain length and solvent dependency may indicate that charge–dipole stabilization makes a greater contribution in the less polar CD_3OH, or solvophobic interactions occur in CD_3OH but are not prevalent in [D_6]DMSO. Indeed, the free N-terminal with a potential positive charge can interact advantageously with the helix macrodipole in the left-handed (M) β-H18 helix, whereas this interaction is disadvantageous for the right-handed (P) β-H12 arrangement. On the other hand, the sequences contain a number of strongly hydrophobic side-chains potentially facilitating solvophobic self-assembly in the protic CD_3OH and head-to-tail helix interactions were also observed for **5**. To address this question, concentration-dependent ECD, DOSY-NMR and transmission electron microscopy (TEM) measurements were performed on **3**–**5**.

The DOSY-NMR results provided direct evidence of the self-assembly processes. The apparent aggregation number converged steeply to a value of 9 for **5**, already reaching a plateau at 100 µM (Fig. 4). TEM image on the 100 µM sample of **5** indicated particles with diameters in the range 6–8 nm (Fig. S14‡), confirming the DOSY findings. For **3** and **4**, the aggregation numbers
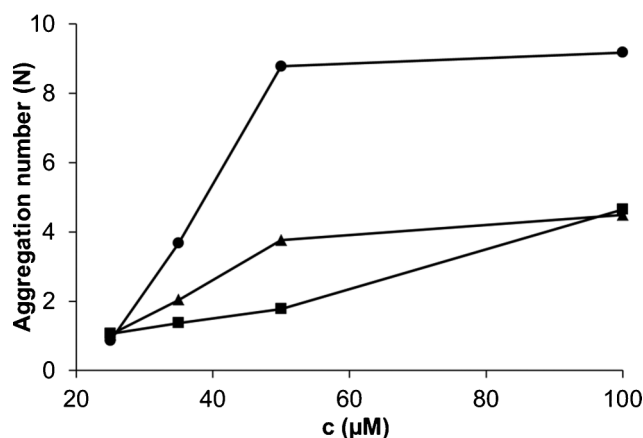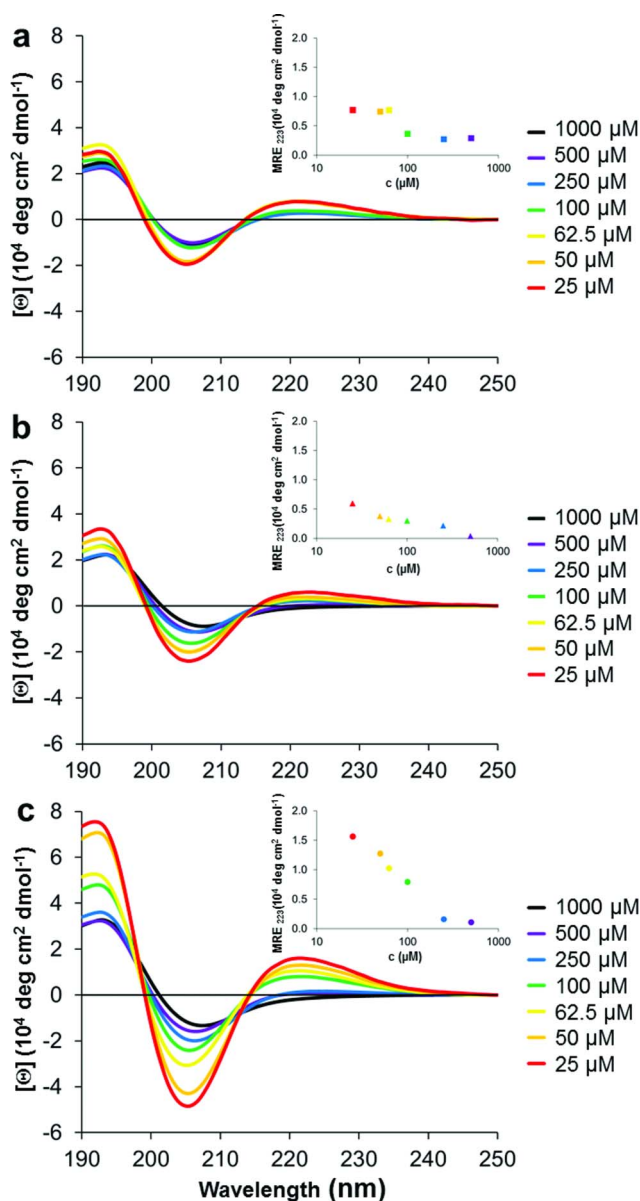

Fig. 4 Concentration-dependent apparent aggregation numbers determined by means of DOSY-NMR for **3** (squares), **4** (triangles) and **5** (circles) in CD_3OH.

increased with lower slopes (Fig. 4), and their behaviour was similar. Self-association was not observed in [D_6]DMSO. These observations suggest that self-assembly plays a role, and further ECD measurements shed light on its effects on the secondary structures.

The analysis revealed concentration-dependent ECD curves (Fig. 5). There was an intensity change for **3**, but the overall ECD fingerprint corresponding to the β-H12 helix remained the same in the concentration range studied. This suggest that the self-assembly has a certain effect on the β-H12 helix of **3**, but is unable to change the overall secondary structure. For **4** and **5**, the Cotton effects clearly changed sign upon dilution; the positive lobes appeared at around 220 nm and the negative lobe exhibited a small blue shift together with a marked intensity change. At lower concentrations the curves converged to the features observed for the β-H12 helix already assigned with the help of **3**. It is important that dilution led to higher-intensity ECD curves, indicating that loss of the interchain interactions results in refolding of the foldamers, but not a disordered state. The self-association correlated well with the H12 → H18 helix transition, and the results strongly suggest that the interchain solvophobic contacts are responsible for the secondary structure change.

Conclusions

Oligomers of *trans*-ABHC and β³-hSer residues were synthesized in the heptamer–nonamer range with various side-chain patterns. It emerged that at least two repulsive contacts of ABHC pairs are necessary in i–i+3 positions to prevent β-H14 helix formation in the heptameric sequences (**1**–**3**). Chain elongation of **3** with ABHC residues resulted in concentration- and solvent-dependent secondary structures for **4** and **5**. In [D_6]DMSO, the β-H12 helix remained stable, whereas CD_3OH as solvent promoted refolding into the β-H18 helix. The role of self-association was tested *via* concentration-dependent ECD and DOSY-NMR measurements. β-H18–β-H12 helix transitions were observed upon dilution of **4** and **5** and the ECD curves revealed that the β-H12 helix becomes predominant at concentrations below 100 µM. The DOSY results confirmed the self-association phenomenon and demonstrated

This journal is © The Royal Society of Chemistry 2012

Org. Biomol. Chem., 2012, **10**, 255–259 | 257

Fig. 5 Concentration-dependent ECD data for **3** (a), **4** (b) and **5** (c) in CH_3OH. The insets depict plots of MRE_{223} *versus* the concentrations (μM) of **3** (squares), **4** (triangles) and **5** (circles). The values were normalized to the chromophore concentration.

a good correlation with the β-H12 → β-H18 helix transition. These observations strongly support the view that foldameric helix refolding is promoted by higher-order packing of the helices in CD_3OH. This system revealed the existence of the β-peptidic H18 helix, a close relative of the α-helix as regards the i–i+4 periodicity of the helix turns, and the helix with the largest diameter to date in the realm of peptidic foldamers.

Acknowledgements

Notes and references

1 D. J. Hill, M. J. Mio, R. B. Prince, T. S. Hughes and J. S. Moore, *Chem. Rev.*, 2001, **101**, 3893–4011.
2 C. M. Goodman, S. Choi, S. Shandler and W. F. DeGrado, *Nat. Chem. Biol.*, 2007, **3**, 252–262.
3 T. A. Martinek and F. Fulop, *Chem. Soc. Rev.*, 2011, DOI: 10.1039/C1CS15097A.
4 S. H. Gellman, *Acc. Chem. Res.*, 1998, **31**, 173–180.
5 R. P. Cheng, S. H. Gellman and W. F. DeGrado, *Chem. Rev.*, 2001, **101**, 3219–3232.
6 W. S. Horne and S. H. Gellman, *Acc. Chem. Res.*, 2008, **41**, 1399–1408.
7 M. A. Schmitt, B. Weisblum and S. H. Gellman, *J. Am. Chem. Soc.*, 2004, **126**, 6848–6849.
8 S. De Pol, C. Zorn, C. D. Klein, O. Zerbe and O. Reiser, *Angew. Chem., Int. Ed.*, 2004, **43**, 511–514.
9 D. H. Appella, L. A. Christianson, I. L. Karle, D. R. Powell and S. H. Gellman, *J. Am. Chem. Soc.*, 1999, **121**, 6206–6212.
10 D. H. Appella, L. A. Christianson, D. A. Klein, M. R. Richards, D. R. Powell and S. H. Gellman, *J. Am. Chem. Soc.*, 1999, **121**, 7574–7581.
11 C. Fernandes, S. Faure, E. Pereira, V. Thery, V. Declerck, R. Guillot and D. J. Aitken, *Org. Lett.*, 2010, **12**, 3606–3609.
12 T. A. Martinek, I. M. Mandity, L. Fulop, G. K. Toth, E. Vass, M. Hollosi, E. Forro and F. Fulop, *J. Am. Chem. Soc.*, 2006, **128**, 13539–13544.
13 A. Hetenyi, G. K. Toth, C. Somlai, E. Vass, T. A. Martinek and F. Fulop, *Chem.–Eur. J.*, 2009, **15**, 10736–10741.
14 R. Threlfall, A. Davies, N. M. Howarth, J. Fisher and R. Cosstick, *Chem. Commun.*, 2008, 585–587.
15 T. D. W. Claridge, J. M. Goodman, A. Moreno, D. Angus, S. F. Barker, C. Taillefumier, M. P. Watterson and G. W. J. Fleet, *Tetrahedron Lett.*, 2001, **42**, 4251–4255.
16 A. Hetenyi, Z. Szakonyi, I. M. Mandity, E. Szolnoki, G. K. Toth, T. A. Martinek and F. Fulop, *Chem. Commun.*, 2009, 177–179.
17 I. M. Mandity, E. Weber, T. A. Martinek, G. Olajos, G. K. Toth, E. Vass and F. Fulop, *Angew. Chem., Int. Ed.*, 2009, **48**, 2171–2175.
18 I. M. Mandity, L. Fulop, E. Vass, G. K. Toth, T. A. Martinek and F. Fulop, *Org. Lett.*, 2010, **12**, 5584–5587.
19 S. H. Gellman, J. L. Price and W. S. Horne, *J. Am. Chem. Soc.*, 2007, **129**, 6376–6377.
20 T. L. Raguse, J. R. Lai, P. R. LePlae and S. H. Gellman, *Org. Lett.*, 2001, **3**, 3963–3966.
21 W. C. Pomerantz, T. L. R. Grygiel, J. R. Lai and S. H. Gellman, *Org. Lett.*, 2008, **10**, 1799–1802.
22 J. X. Qiu, E. J. Petersson, E. E. Matthews and A. Schepartz, *J. Am. Chem. Soc.*, 2006, **128**, 11338–11339.
23 D. S. Daniels, E. J. Petersson, J. X. Qiu and A. Schepartz, *J. Am. Chem. Soc.*, 2007, **129**, 1532–1533.
24 E. J. Petersson, C. J. Craig, D. S. Daniels, J. X. Qiu and A. Schepartz, *J. Am. Chem. Soc.*, 2007, **129**, 5344–5345.
25 J. L. Goodman, E. J. Petersson, D. S. Daniels, J. X. Qiu and A. Schepartz, *J. Am. Chem. Soc.*, 2007, **129**, 14746–14751.
26 T. Wieprecht, O. Apostolov, M. Beyermann and J. Seelig, *J. Mol. Biol.*, 1999, **294**, 785–794.
27 T. Wieprecht, M. Beyermann and J. Seelig, *Biophys. Chem.*, 2002, **96**, 191–201.
28 K. Sakajiri, K. Satoh, S. Kawauchi and J. Watanabe, *J. Mol. Struct.*, 1999, **476**, 1–8.
29 K. Otoda, Y. Kitagawa, S. Kimura and Y. Imanishi, *Biopolymers*, 1993, **33**, 1337–1345.
30 R. S. Vieira-Pires and J. H. Morais-Cabral, *J. Gen. Physiol.*, 2010, **136**, 585–592.
31 G. Yoder, A. Polese, R. A. G. D. Silva, F. Formaggio, M. Crisma, Q. B. Broxterman, J. Kamphuis, C. Toniolo and T. A. Keiderling, *J. Am. Chem. Soc.*, 1997, **119**, 10278–10285.
32 M. Bellanda, S. Mammi, S. Geremia, N. Demitri, L. Randaccio, Q. B. Broxterman, B. Kaptein, P. Pengo, L. Pasquato and P. Scrimin, *Chem.–Eur. J.*, 2007, **13**, 407–416.

33 A. Hayen, M. A. Schmitt, F. N. Ngassa, K. A. Thomasson and S. H. Gellman, *Angew. Chem., Int. Ed.*, 2004, **43**, 505–510.

34 A. Hetenyi, I. M. Mandity, T. A. Martinek, G. K. Toth and F. Fulop, *J. Am. Chem. Soc.*, 2005, **127**, 547–553.

35 Z. Szakonyi, T. A. Martinek, R. Sillanpaa and F. Fulop, *Tetrahedron: Asymmetry*, 2008, **19**, 2296–2303.

36 T. S. Li, T. Horan, T. Osslund, G. Stearns and T. Arakawa, *Biochemistry*, 1997, **36**, 8849–8857.

37 D. Seebach, J. V. Schreiber, S. Abele, X. Daura and W. F. van Gunsteren, *Helv. Chim. Acta*, 2000, **83**, 34–57.

38 S. H. Choi, I. A. Guzei, L. C. Spencer and S. H. Gellman, *J. Am. Chem. Soc.*, 2008, **130**, 6544–6550.

39 G. L. Millhauser, *Biochemistry*, 1995, **34**, 3873–3877.

40 N. H. Andersen, J. W. Neidigh, S. M. Harris, G. M. Lee, Z. H. Liu and H. Tong, *J. Am. Chem. Soc.*, 1997, **119**, 8547–8561.

41 www.gaussian.com.

42 T. Beke, I. G. Csizmadia and A. Perczel, *J. Comput. Chem.*, 2004, **25**, 285–307.

43 K. Mohle, R. Gunther, M. Thormann, N. Sewald and H. J. Hofmann, *Biopolymers*, 1999, **50**, 167–184.

This journal is © The Royal Society of Chemistry 2012

Org. Biomol. Chem., 2012, **10**, 255–259 | 259